Modeling of Selective Interruption Using Coordination Capacitor and Solid-State Circuit Breakers in Urban DC Microgrids

Naoki Hanaoka, Naruto Arai, Toshihiro Hayashi
Space Environment and Energy Laboratories
NTT, Inc.
Tokyo, Japan
naoki.hanaoka@ntt.com

***Abstract*—This paper proposes a fundamental simulation model to evaluate the scalability of a selective-interruption method combining a coordination capacitor with solid-state circuit breakers (SSCBs) in DC microgrids. The model reproduces fault behavior on a feeder comprising a DC source, line impedance, SSCBs, and a coordination capacitor inserted between SSCBs. Comparison with experimental results validated the proposed method, which showed sufficiently small error in current-waveform peak and timing. Simulation analyses were then performed to investigate how varying the coordination-capacitor value affects the upstream fault-current peak and selective-interruption performance. The results demonstrate that the coordination capacitor functions as a practical current-supplying element, promoting the downstream SSCB to trip first while suppressing fault current through the upstream SSCBs. This protection approach, physically combining a coordination capacitor with SSCBs, enhances protection coordination, operational reliability, and system resilience in urban DC microgrids supplying power to critical digital infrastructure facilities such as datacenters and telecommunication buildings.**

***Index Terms*—DC microgrid, fault protection, selective interruption, smart grid, solid-state circuit breaker**

I. INTRODUCTION

Urban digital infrastructure—such as telecommunication buildings and datacenters—adopts a 380-V DC distribution in selected installation to enhance reliability and availability [1]. In city-scale microgrids, ring topologies effectively share feeders and improve voltage profiles. However, because the current direction within the ring is not fixed, conventional circuit breakers can achieve selective interruption for the predesigned current direction but not for the reverse direction [2]–[4]. Recent literature covers ring-microgrid protection using parameter estimation or transient-feature methods [3], [4] and solid-state circuit breakers (SSCB) based protection in DC systems including shipboard distribution [2].

We previously demonstrated experimentally that, in a circuit consisting of two series-connected SSCBs with identical trip thresholds, inserting a coordination capacitor between them enables selective interruption (protection coordination) [5]. The coordination capacitor supplies additional fault current from the capacitor to the downstream SSCB during a fault, thereby promoting rapid tripping of the SSCB near the fault point while preventing unintended tripping of the upstream SSCB. Another study has reported a combination of capacitors and SSCBs [6]. In that case, however, the capacitor was connected in parallel with the breaker to limit the voltage rise across the mechanical contacts during switching. Therefore, the combination's purpose and operating mechanism differ from those in this study.

In our laboratory-scale experiments using prototype devices, it was difficult to demonstrate the scalability of the selective-interruption method that combines a coordination capacitor and SSCBs [5]. Therefore, verifying its scalability through simulation remained a key challenge. This paper aims to model a fundamental simulation that serves as an analytical foundation for future research.

II. SYSTEM CONFIGURATION AND FAULT PROTECTION METHOD

Fig. 1 illustrates ring-type DC microgrid layouts for telecom and datacenter clusters. We use a rated voltage of 380 V for the main line because this standardized level [7] ensures compatibility with existing DC systems. The internal DC bus of each building is connected to the ring wiring through a DC/DC converter. The ring wiring is assumed to operate as an independent system separated from the main grid. The device that connects a coordination capacitor at the junction of three SSCBs is installed at the intersection between the main line and the branch line. The blue squares in Fig. 1 represent the SSCBs, and the white arrows indicate the directions of current measurement. These systems form part of urban digital infrastructures that demand high reliability and rapid fault isolation. The ring configuration offers redundant power-flow paths but also introduces challenges in coordinating the operation of SSCBs under bidirectional current conditions.

On the basis of this system configuration, the protection scheme forces only the breaker closest to the fault to open, while the upstream breakers keep conducting to sustain power delivery to non-faulted sections. When a fault occurs in the ring wiring, additional fault current is supplied from not only each DC/DC converter but also the coordination capacitor, enabling the SSCB located nearest to the fault point to be selectively interrupted. The effectiveness of the coordination capacitor has been experimentally demonstrated, although on a limited scale [5].

979-8-3315-8138-1

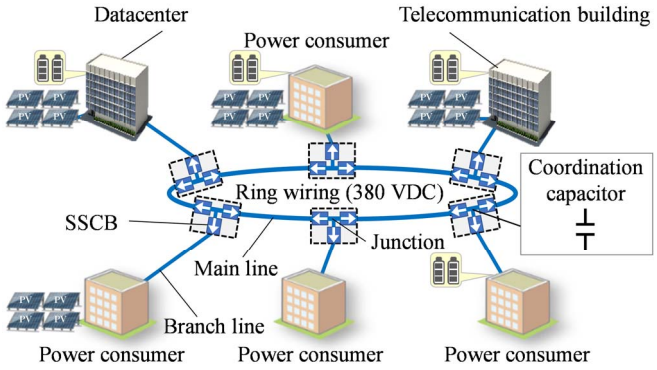

Figure 1. Example of a ring-type DC microgrid configuration centered around communication buildings and datacenters.

This fault protection scheme addresses the protection challenges reported in recent DC microgrid studies under bidirectional power flow conditions [2], [8]. In addition, because it can selectively isolate the faulted section within a short time, it is well suited for DC microgrids connecting telecommunication buildings and datacenters [1], where continuous power supply, high reliability, and resilience against faults are essential.

III. Model Development and Circuit Description

To develop the simulation model, we validated its accuracy by comparing it with previously obtained experimental results.
Section A describes the experimental conditions from the earlier study, and Section B presents the corresponding conditions of the simulation model.

A. Experimental Setup

Fig. 2 shows the experimental circuit that we built as the basis for the simulation model. We connected two SSCBs (SSCB1 and SSCB2) in series through line impedances and inserted a coordination capacitor between them, assuming that if selective interruption can be achieved between the SSCB closest to the fault point and the immediately upstream SSCB, the upstream SSCBs will not trip. In constructing the base simulation, the experimental setup was simplified as much as possible, and the line impedance was set equivalent to that of a 1-m cable. Since increasing the line impedance makes selective interruption between SSCBs easier in the intended DC microgrid, the line impedance was reduced to represent the worst-case condition. We simulated a fault experimentally by closing a fault switch downstream of SSCB2 to evaluate the protection behavior. We defined successful coordination as the condition in which only SSCB2 opened, while SSCB1 continued to conduct. In the preliminary experiments, SSCB2 operated normally in all test cases. The current waveform of SSCB1 during a fault was measured, and the effect of the coordination capacitor's capacitance was examined. Therefore, the modeling in this paper focused on the current of SSCB1. Details of the relevant experiments are summarized in [5].

The SSCB prototype used in the experiment, developed on the basis of [9], is shown in Fig. 3. The SSCB circuit is housed inside the black enclosure. It operates at a rated voltage of 380

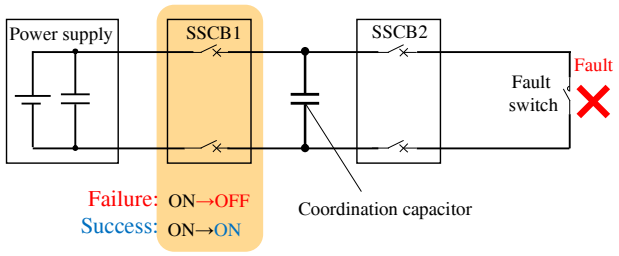

Figure 2. Simplified experimental circuit used as the basis of the simulation model.

V DC and trips when the current reaches the preset threshold.

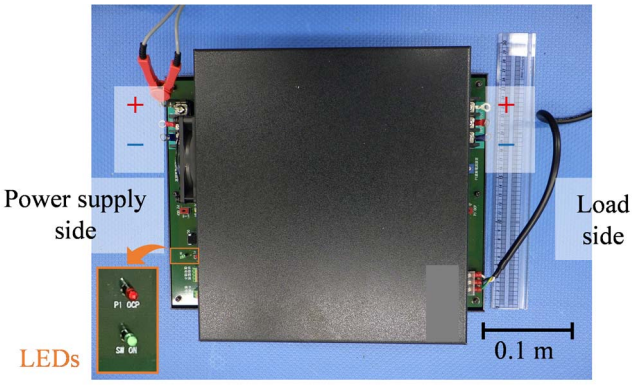

Figure 3. Photograph of the solid-state circuit breaker (SSCB) used in the experiments.

The tripping event can be visually confirmed through the LED indicator. In this experiment, the trip threshold of the SSCB was set to 30 A, as the system was designed to simulate a power level of approximately 10 kW for power transmission and reception.

B. Simulation Model

Fig. 4 shows the power electronics circuit simulator (PSIM) based simulation circuit reproducing the fault experiment. Fig. 4(a) shows a simulation model that reproduces the fault experimental system, in which two SSCBs are connected in series through line impedances, and a coordination capacitor is inserted between them. Fig. 4 (b) shows the internal simulation model of the SSCB, consisting of voltage-controlled semiconductor switches, free-wheel diodes, and RC snubber networks that reproduce the transient behavior during interruption. A fault condition is simulated by closing a fault switch at the fault point to analyze the selective interruption performance.

The parameters used in the simulation circuit in Fig. 4 are summarized in Table I. As shown, the circuit assumes a 380 V DC bus with a 30 A trip threshold for both SSCBs. To enable the simulation and experimental results to be directly compared, the model uses laboratory-level line impedances. The coordination capacitor is varied from 50 to 300 µF to investigate its influence on the current distribution and protection coordination.

The scope of this simulation model is as follows. Each SSCB is modeled with only the essential elements required for fault studies; not all internal submodules are represented. The

model focuses on fault conditions, and other operating events (e.g., ground fault, high-resistance fault) are beyond its scope.

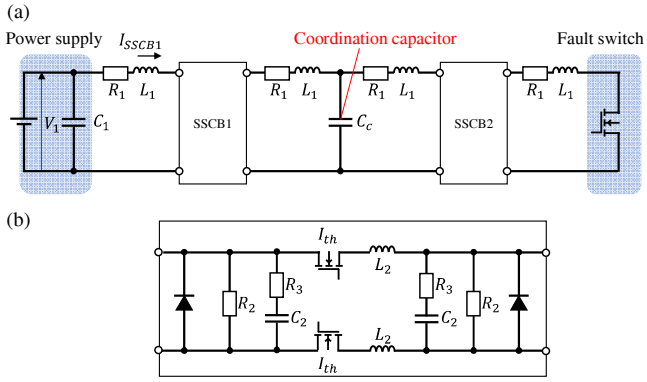

Figure 4. Simulation circuit diagram: (a) fault experimental system model and (b) SSCB internal circuit model.

TABLE I. CIRCUIT PARAMETERS USED IN THE SIMULATION MODE.

Symbol	*Description*	*Value*
V_1	DC power supply voltage	380 V DC
I_{th}	Trip threshold current of SSCB1 and SSCB2	30 A
R_1	Line resistance between nodes	1 mΩ
R_2	High-value resistor	99 kΩ
R_3	RC snubber circuit	30 Ω
L_1	Line inductance between nodes	1 µF
L_2	Current-limiting inductor	50 µF
C_1	X capacitor of power supply	2000 µF
C_2	RC snubber circuit	0.1 µF
C_c	Coordination capacitor	50 – 300 µF (step 50 µF)

IV. RESULTS AND VALIDATION

A. Model Validation

Fig. 5 shows the SSCB1 current I_{SSCB1}, where the simulation waveform is overlaid with the experimental results. In both the experimental and simulation systems, a fault is initiated at $t = 0$ ms. This case corresponds to the condition without a coordination capacitor ($C_c = 0$ µF). The measurement error of the current transformer (CT) is ±0.03%. The peak current reached 31.500 A in the experiment and 30.005 A in the simulation, both slightly exceeding the 30 A threshold. The peak is 4.75% lower and appears 0.0456 ms later in the simulation than in the experiment. However, the peak value of the experimental waveform may have been affected by noise superimposed during the tripping event. When this noise is excluded, the peak current in the experiment becomes 30.375 A, 1.22% lower than in the simulation. The 0.0456 ms difference is minor and is considered to barely impact the selective-interruption method, since both SSCBs in the simulation show the same delay

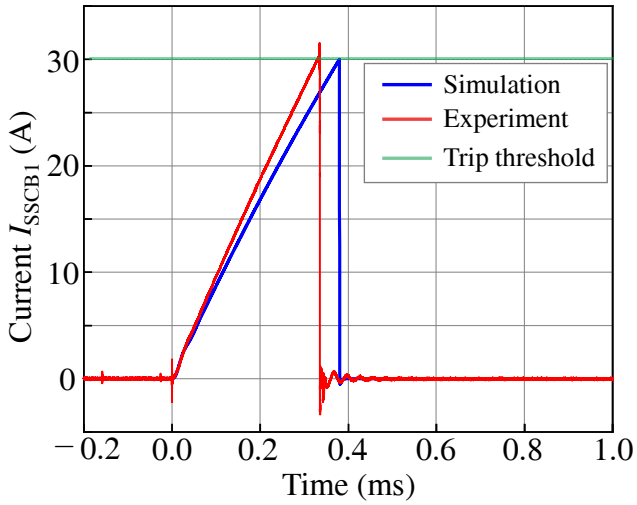

Figure 5. SSCB1 input-current at a fault: simulation vs. experiment.

relative to the experimental results. This close agreement validates the fault-oriented SSCB model and demonstrates that the adopted line-impedance representation appropriately reproduces the experimental behavior for coordination analysis.

B. Coordination Capacitor Sensitivity

Our previous fault experiments demonstrated the effectiveness of the coordination capacitor. To verify whether the developed simulation model can also reproduce this effectiveness, a parameter sensitivity analysis of the coordination capacitor was conducted.

Fig. 6 shows six simulated waveforms of the SSCB1 input current for C = 50, 100, 150, 200, 250, and 300 µF. Table II quantifies the peak current of SSCB1 as a function of the coordination capacitor value. From 50 to 300 µF, the peak current decreases by 9% from 30.010 to 27.193 A. For capacitances of 50 µF, the current through SSCB1 exceeded 30 A, causing SSCB1 to trip; therefore, the current dropped to 0 A around 0.35 ms. In contrast, for capacitances between 100 and 300 µF, SSCB1 did not trip, and the current decreased gradually over time.

As shown, as the capacitance increases, the peak fault current of SSCB1 decreases monotonically. The current margin to the 30 A trip threshold increases as capacitance increases. The ratio column highlights that when C ≥ 100 µF, the SSCB1 current remains below the trip limit, indicating coordination with the downstream breaker. These results indicate that as the capacitance of the coordination capacitor increases, the fault current I_{p_SSCB1} supplied from the upstream source to SSCB1 decreases. The total fault current I_s is the sum of the source current I_{p_SSCB1} and the capacitor current I_c. Since I_s is nearly constant at approximately 30 A, determined by the tripping threshold of SSCB2, a decrease in I_{p_SSCB1} implies a corresponding increase in I_c. Therefore, the coordination capacitor functions as a current source during a

fault, supplying additional current I_c toward the downstream

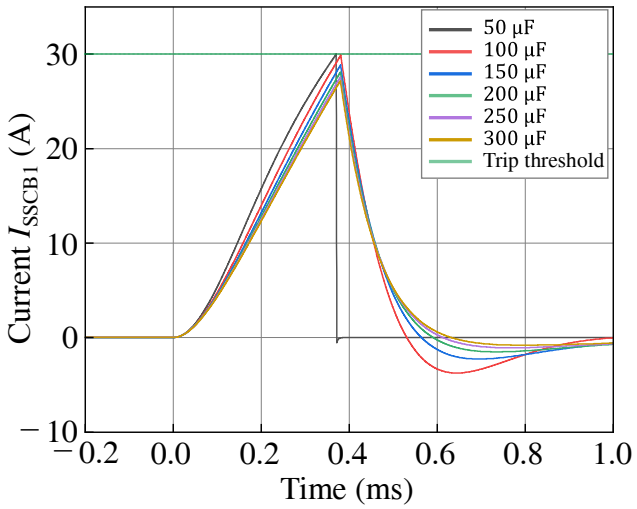

Figure 6. SSCB1 input current for different coordination-capacitor values.

SSCB2 and enabling selective interruption.

TABLE II. PEAK CURRENT OF SSCB1 VS. COORDINATION CAPACITOR.

Cc [µF]	I_{P_SSCB1} [A]	*Margin to 30A*	
		Current[a] [A]	*Ratio*[b] [%]
50	30.010	+0.010	100.033
100	29.899	−0.101	99.663
150	28.875	−1.125	96.250
200	28.135	−1.865	93.783
250	27.590	−2.410	91.966
300	27.193	−2.807	90.643

a. Negative margins indicate below the 30 A threshold.

b. The value obtained by dividing the peak current flowing through SSCB1 by 30 A.

V. DISCUSSION AND CONCLUSION

The ring-type topology is attractive for urban DC microgrids that interconnect telecom buildings and datacenters. Still, selectivity becomes difficult when the fault current direction varies with fault location. Methods based on parameter estimation or transient features can realize selectivity but often require communication, detailed line models, or complex signal processing [3], [4], [10]. In contrast, the proposed method physically combines a coordination capacitor with solid-state circuit breakers (SSCBs), providing a practical tuning parameter that allows the fault current distribution to be controlled. By adjusting the capacitor value, the upstream SSCBs remain below their trip thresholds while the downstream breaker operates first and clears the fault within a few milliseconds.

Recent studies have focused on SSCB implementations and DC-microgrid fault detection techniques—such as bidirectional-thyristor SSCBs, ΔV–ΔI plane-based fault detection, and microgrid islanding protection—reflecting a strong research interest in fast, device-level protection and selectivity [11]–[13]. For higher-voltage systems, fast protection of HVDC grids using transient features has also been widely investigated [14]. Our new proposal in this study is a selective-interruption method using SSCBs and a coordination capacitor for low-voltage DC microgrids, which may complement or provide an alternative to existing methods.

We developed and validated a circuit simulation model for selective interruption in DC microgrids, employing two series-connected SSCBs and a coordination capacitor. Increasing the capacitor value effectively reduces the upstream fault current peak while increasing the likelihood that only the breaker closest to the fault operates, as observed in simulation waveforms from a 380-V test setup. This study contributes to enhancing fault-protection strategies in urban DC microgrids that supply critical digital infrastructure, such as datacenters and telecommunication buildings. Moreover, by maintaining service continuity under fault conditions, the proposed coordination-capacitor-based protection contributes to improving the overall resilience of urban DC microgrids.

Future work will extend and refine the model to larger-scale network configurations and examine coordination behavior over longer feeders. These findings provide a scalable foundation for developing coordination-capacitor-based protection schemes in future DC microgrid architectures.

REFERENCES

[1] T. Tanaka, N. Hanaoka, A. Takahashi, K. Asakimori, T. Iwato, A. Sakurai, and N. Yamashita, “Concept of new power supply system topology using 380 V and 48 V DC bus for future datacenters and telecommunication buildings,” in Proc. IEEE INTELEC, Oct. 2015, pp. 1–6, doi: 10.1109/INTLEC.2015.7572379.

[2] L. Qi, P. Cairoli, Z. Pan, et al., “Solid-State Circuit Breaker protection for DC shipboard power systems: breaker design, protection scheme, validation testing,” IEEE Trans. Ind. Appl., 2020.

[3] R. Mohanty and A. K. Pradhan, “Protection of smart DC microgrid with ring configuration using parameter estimation approach,” IEEE Trans. Smart Grid, vol. 9, no. 6, pp. 6328–6337, Nov. 2018, doi: 10.1109/TSG.2017.2708743.

[4] R. Mohanty and A. K. Pradhan, “DC ring-bus microgrid protection using the oscillation frequency and transient power,” IEEE Systems Journal, vol. 13, no. 1, pp. 875–884, Mar. 2019, doi: 10.1109/JSYST.2018.2837748.

[5] N. Hanaoka, Y. Higuchi, N. Arai, and K. Akiyama, “Protection coordination of semiconductor circuit breakers in ring-type 380-V DC microgrid,” Energy Proceedings (ICAE 2024), vol. 49, 2024, doi: 10.46855/energy-proceedings-11388.

[6] D. Jovcic, “Multibreak LC DC circuit breaker,” in Proc. IEEE PES General Meeting (PESGM), 2022, pp. 1–5, doi: 10.1109/PESGM48719.2022.9916775.

[7] International Telecommunication Union (ITU-T), Recommendation ITU-T L.1200: Direct current power feeding interface up to 400 V at the input to telecommunication and ICT equipment, Geneva, Switzerland, Apr. 2012. [Online]. Available: https://www.itu.int/rec/T-REC-L.1200/en

[8] A. Pogulaguntla, G. V. Yagna, S. N. Banavath, and R. Singh, “A thyristor-controlled bidirectional DC solid-state circuit breaker for residential microgrids,” in Proc. IEEE PESGM, 2024, p. 1827 (Program ToC pagination).

[9] K. Murai, T. Tanaka, T. Babasaki, and Y. Nozaki, “Improvement of PDC and PDU with semiconductor breakers,” in Proc. IEEE INTELEC, 2012, doi: 10.1109/INTLEC.2012.6374466.

[10] S. K. Maurya, R. K. Panda, A. Mohapatra, and A. Sharma, “ΔV−ΔI plane-based line faults detection and classification in DC microgrid,” in Proc. IEEE PESGM, 2024, p. 1932 (Program ToC pagination).

[11] R. Jafari, B. F. Yancey, S. Bye, G. Yakle, and A. Meissner, “Utility-scale BESS/PV microgrid islanding challenges and protection considerations,” in Proc. IEEE PESGM, 2024, p. 1837 (Program ToC pagination).

[12] R. Peykarporsan, T. T. Lie, M. Stommel, and J. Watson, “Model order reduction for control and stability analysis of complex dynamical systems in a DC microgrid,” in Proc. IEEE PESGM, 2024, p. 1196 (Program ToC pagination).

[13] L. He, G. Meghwar, and S. Yu, “An enhanced fault detection strategy based on the transient voltage in multi-terminal HVDC grid,” in Proc. IEEE PESGM, 2024 (Best Paper selection news).

[14] S. Kumar et al., “Protection techniques for DC microgrid—A review,” Electric Power Systems Research, vol. 189, 2020, Art. 106602.